IEEE Access
Multidisciplinary | Rapid Review | Open Access Journal

Received 6 February 2024, accepted 11 March 2024, date of publication 20 March 2024, date of current version 26 March 2024.

Digital Object Identifier 10.1109/ACCESS.2024.3379136

RESEARCH ARTICLE

Optimized Brain Tumor Detection: A Dual-Module Approach for MRI Image Enhancement and Tumor Classification

ABDULLAH A. ASIRI[1], TOUFIQUE AHMED SOOMRO[2], (Senior Member, IEEE), AHMED ALI SHAH[3], (Senior Member, IEEE), GANNA POGREBNA[4,5,6], MUHAMMAD IRFAN[7], AND SAEED ALQAHTANI[1]

[1]Radiological Sciences Department, College of Applied Medical Sciences, Najran University, Najran 61441, Saudi Arabia
[2]Department of Electronic Engineering, The University of Larkano (UOL), Larkana 77111, Pakistan
[3]Electrical Engineering Department, Sukkur IBA University, Sukkur 65200, Pakistan
[4]Artificial Intelligence and Cyber Futures Institute, Charles Sturt University, Bathurst, NSW 2795, Australia
[5]The University of Sydney Business School, The University of Sydney, Darlington, NSW 2006, Australia
[6]The Alan Turing Institute, NW1 2DB London, U.K.
[7]Electrical Engineering Department, College of Engineering, Najran University, Najran 61441, Saudi Arabia

Corresponding author: Toufique Ahmed Soomro (etoufique@yahoo.com)

This work was supported by the Deanship of Scientific Research, Najran University, Kingdom of Saudi Arabia, for funding this work through the National Research Priorities and Najran Area Funding Program, under Grant NU/NRP/MRC/12/26.

ABSTRACT Neurological and brain-related cancers are one of the main causes of death worldwide. A commonly used tool in diagnosing these conditions is Magnetic Resonance Imaging (MRI), yet the manual evaluation of MRI images by medical experts presents difficulties due to time constraints and variability. This research introduces a novel, two-module computerized method aimed at increasing the speed and accuracy of brain tumor detection. The first module, termed the Image Enhancement Technique, utilizes a trio of machine learning and imaging strategies—adaptive Wiener filtering, neural networks, and independent component analysis—to normalize images and combat issues such as noise and varying low region contrast. The second module uses Support Vector Machines to validate the output of the first module and perform tumor segmentation and classification. Applied to various types of brain tumors, including meningiomas and pituitary tumors, our method exhibited significant improvements in contrast and classification efficiency. It achieved an average sensitivity and specificity of 0.991, accuracy of 0.989, and a Dice score (DSC) of 0.981. Furthermore, the processing time of our method, averaging at 0.43 seconds, was markedly lower compared to existing methods. These results underscore the superior performance of our approach over current state-of-the-art methods in terms of sensitivity, specificity, precision, and DSC. Future enhancements will seek to increase the robustness of the tumor classification method by employing a standardized approach across a suite of classifiers.

INDEX TERMS Magnetic resonance imaging (MRI), image enhancement technique, brain tumor segmentation, neural networks, brain tumor classification.

I. INTRODUCTION

Brain abnormalities, commonly referred to as tumors in medical terminology, are classified as malignant or benign. There are approximately 200 different types of brain tumors that can occur in various regions of the human brain. These tumors can have a significant and often life-changing impact on individuals' lives. Numerous studies provide strong scientific evidence of increasing brain tumor incidence and its association with human mortality [1]. According to the

The associate editor coordinating the review of this manuscript and approving it for publication was Yi Zhang.

American Cancer Society, brain tumor is one of the serious diseases in which the brain tissues are increased irregularly and affects the brain function. The research was conducted by the National Brain Tumor Foundation, and they reported that the number of people who have lost their lives to brain tumors has increased by 300% over the past three decades. Treatment is necessary, otherwise brain tumors could lead to death if left untreated [2]. The physical appearance of the brain and the complexity of brain tumors pose challenges for health care to diagnose and recommend early treatment to the patient. Early detection of brain tumors and proper treatment play an important role in improving the survival rate of patients. Because biopsy of a brain tumor is not such a simple task as biopsy of other parts of the body, as it must necessarily be performed with surgical intervention. SO. This requires the most effective methods to diagnose brain tumor without surgery and many imaging modalities are used, but magnetic resonance imaging (MRI) is the best option and it is commonly used to diagnose brain tumors [3], [4].

Brain MRI imaging utilizes a range of techniques to acquire data, which is subsequently processed to form input vectors for classification purposes, and MRI imaging filters are used to identify brain tumors and help the radiologist recommend treatment. The radiologist has two types of choices for identifying brain tumors. First, they distinguish between typical or normal brain MRI images, and second, they classify brain MRI images into different brain tumor types. Brain MRI images are the most important symptomatic neuroimaging testing device that identifies baseline variations from norms in the brain. This is particularly crucial for the diagnosis and monitoring of brain tumors, as MRI scans can accurately detect and characterize tumors, assess their growth over time, and aid in treatment planning [5], [6]. Brain MRI images are used to diagnose brain abnormalities, including those that may indicate the presence of a brain tumor [9]. MRI provides detailed images of the brain and is one of the most common tests used to identify brain tumors. MR images provide the soft tissues of the human body, and these images are mainly used to detect brain structure and function [7], [8]. In this research work, we have proposed enhancement method to solve the contrast problem of brain MRI images, and this leads to give accurate identification of brain tumor.

The main objective of this research work is to understand brain MRI images and to solve the problem of low contrast variation of these images which leads to segmenting the tumor and classifying normal and abnormal images. Brain MRI image analysis is challenging due to issues like noise, resolution, contrast, motion artifacts, variability, and complex brain structures. Our proposed method is based on new implementations of contrast enhancement techniques and its impact on segmentation and classification. Image enhancement techniques solve the three problems of brain MRI images, and the first problem is noise suppression, and the second problem is the resolution of low contrast and varying contrast and the last step is based on coherence of the image contrast. We used the adaptive Wiener filter with neural networks to normalize the image contrast. Then, we used an independent component analysis to even out the contrast and obtain a well-contrasted image. This enhancement technique is validated on the CE-MRI database and its impact on the classification of brain tumors has also been observed. The novelty of the proposed method lies in its innovative application of contrast enhancement techniques, including the use of the adaptive Wiener filter, neural networks, and independent component analysis,it aims to produce clearer, more consistent, and well-contrasted MRI images, thereby improving the accuracy of tumor segmentation and classification. The proposed method contributes to the field of brain MRI image analysis in several significant ways:

1) **Contrast Enhancement Techniques**: The method introduces innovative implementations of contrast enhancement techniques, including the use of the adaptive Wiener filter, neural networks, and independent component analysis, to address the challenge of low-contrast MRI images.
2) **Validation on CE-MRI Image Database**: The method's effectiveness is validated on the CE-MRI image database, providing evidence of its practical application and impact on the accurate classification of brain tumors.
3) **Innovation in MRI Enhancement**: The proposed method's novelty lies in its innovative application of contrast enhancement techniques, offering a fresh approach to addressing the specific challenges of MRI images.
4) **Improved Accuracy**: By producing clearer, more consistent, and well-contrasted MRI images, the method ultimately aims to enhance the accuracy of tumor segmentation and classification, contributing to more reliable clinical diagnoses.

The proposed method's contributions include addressing the challenges of low-contrast MRI images, noise suppression, resolution enhancement, coherence improvement, and validation on a relevant database. These contributions collectively improve the accuracy of brain tumor segmentation and classification, which is valuable in clinical and medical imaging contexts.

II. RELATED WORK

The early detection of brain tumors is crucial for effective treatment, and various methods have been explored by researchers [10] to achieve this goal. Selvapandian and Manivannan [11] used the non-subsampled contourlet transform (NSCT) to enhance brain images and extract surface features, followed by adaptive neural techniques for classification and glioma brain tumor area segmentation. While their approach addressed important aspects of the problem, specific performance metrics for their methodology were not provided, leaving room for further evaluation.

In a different approach, Sharif et al. [12] introduced a technique for skull section removal from brain images using brain surface extraction (BSE) and particle swarm

optimization (PSO) for segmentation. This method achieved an impressive maximum accuracy of 99% when evaluated on complex brain datasets, indicating its potential for accurate brain tumor detection. However, it's important to note that this method may not have addressed other types of brain tumors or potential performance issues in different scenarios. Kumar et al. [13] proposed the Weighted Correlation Feature Selection Based Iterative Bayesian Multivariate Deep Neural Learning (WCFS-IBMDNL) method, which combines feature selection with Iterative Bayesian Multivariate Deep Neural Network (IBMDNN) classification to identify brain tumors. While this method offers an integrated approach, it exhibited high False Alarm Rates (FARs), suggesting that there is room for improvement in terms of accuracy and reducing false positives.

Ozyurt et al. [14] took a mixed approach, combining eutrosophy and Convolutional Neural Network (CNN) with Neutrosophy to categorize malignant and benign tumor regions in brain images. Their method achieved an impressive average success rate of 95.62% through the use of CNN features and SVM for classification. However, the choice of CNN features may not be universally optimal for all types of brain tumors, and further exploration of feature selection could enhance the method's versatility. In another study, Raju et al. [15] utilized a computerized method based on a multi-class Support Vector Neural Network (SVNN) trained with the Harmony-Crow Search (HCS) optimization technique for tumor identification in MRI images. However, this method solely relied on the BRATS dataset for evaluation, potentially limiting its generalizability to a broader range of cases. Researchers and practitioners should carefully consider the specific requirements of their brain tumor detection tasks when choosing among these methods, considering factors such as the type of tumor, available datasets, and the desired balance between accuracy and computational complexity.

Yin et al. [16] explored background elimination, feature extraction, and classification phases using multilayer perceptron networks, incorporating techniques like the Whale Optimization Algorithm and chaos theory for feature selection and classification. However, their algorithm did not significantly enhance accuracy. In contrast, Krol and Gimi [17] employed deep learning with a substantial MRI image dataset, using dual neural networks (fully connected and CNNs) to classify brain images with tumors, achieving an impressive 91.43% accuracy via 5-fold cross-validation. Similarly, Mittal et al. [18] presented an MRI-based brain tumor identification method that automated segmentation with a Growing Convolution Neural Network (GCNN) and Stationary Wavelet Transform (SWT). This approach outperformed other methods, including CNN, SVM, and KNN, in terms of accuracy [18], [19].

Rehman et al. [20] used VGGNet, GoogLeNet, and AlexNet CNNs to distinguish between three types of brain tumors. They employed data augmentation to prevent overfitting and boost the sample size, with VGG16 achieving an outstanding accuracy of 98.69%, the highest among the compared methods. Another study [21] used a two-stage strategy to distinguish healthy brains from those with tumors, employing CNNs for preprocessing and Error-Correcting Output Codes SVM (ECOCSVM) for classification in the second stage. Impressively, AlexNet achieved the highest accuracy at 99.55%. The evaluation was conducted using the BraTS and RIDER databases.

Abiwinanda [22] utilized a CNN to detect common brain tumors, achieving high training and validation accuracy rates of 98.51% and 84.19%, respectively, with a dataset of 3064 T-1 weighted CE-MRI images. Pashaei et al. [23] proposed a CNN-based model for identifying meningioma, glioma, and pituitary tumors, achieving an accuracy of 93.68% and comparing their method with other models using ten-fold cross-validation. In Gumaei et al. [24] study, involving preprocessing, feature extraction, and classification, they achieved an accuracy of 94.23% with Principle Component Analysis Normalized GIST (PCA-NGIST) and Regularized Extreme learning machine (RELM), though they did not conduct a comparative analysis with previously reported techniques.

Phaye et al. [25] introduced DCNet++ and DCNet as techniques for brain tumor classification, attaining accuracy values of 95.03% and 93.04%, respectively, using MRI images. However, a drawback was the absence of a dataset representing healthy individuals for classification, limiting the context of the results. Badža and Barjaktarovic [26] presented a CNN-based method with 22 layers designed for the classification of pituitary, meningioma, and glioma tumors, achieving an impressive accuracy of 96.56% through k-fold cross-validation. Sharma et al. [27] adopted a hybrid approach that combined Artificial Neural Networks (ANN) and K-means clustering for tumor classification. Their method featured efficient tumor region identification through GLCM-based feature extraction and k-means algorithm integration, which was a notable strength. Rani et al. [28] employed SVM for brain tumor classification, complemented by Otsu thresholding. However, comparative studies revealed the potential for accuracy improvement in their method. To meet the demand for enhanced brain tumor detection algorithms, Molina-Torres [29] employed a kernel SVM approach, specifically the Gaussian Radial Basis (GRB) kernel, focusing on metrics such as specificity, precision, and accuracy, which provided valuable insights into algorithm performance.

In conclusion of analysing the existing work, the body of research reviewed in this section represents a significant advancement in the field of brain tumor detection and classification. These studies have explored various techniques, ranging from deep learning and CNNs to hybrid approaches and SVMs, achieving promising results in terms of accuracy and classification performance. However, it is important to acknowledge the existing gaps and limitations, including

the need for more comprehensive datasets, comparative analyses, and improvements in the consistency of evaluation metrics. These insights provide a solid foundation for the proposed methods and approaches that will be discussed in the subsequent sections, aiming to further refine and enhance the state-of-the-art in brain tumor detection using MRI images.

III. PROPOSED METHOD

Brain MRI images are used in our proposed method as it is a non-invasive process and it provides us with the multidimensional analysis as compared to other modalities such as CT scan and X-ray images. The main purpose of brain MRI images is to identify the brain tumor and classify its precise region. Before performing segmentation and classifications of brain MRI images, it is necessary to improve image contrast as well as reduce noise. In this research work, we propose image enhancement techniques as well as the analysis of its impact on the segmentation of the abnormal region. The proposed methodology is illustrated in the Figure 1

The main theme of the implementation of the proposed method to identify the abnormal region as a tumor from brain MRI images. In the proposed technique as shown in Figure 1. It is a computerized method of brain tumor detection, and it depends on the noise-free trained image of brain MRI images and then it is processed to enhance the image using independent component analysis. The image enhancement technique for brain MRI images is implemented in this research work and its impact is validated on the post-processing steps that lead to obtaining the brain tumor. The different steps of image enhancement techniques for brain tumors as well as brain tumor detection are elaborated in the following sections.

A. STEP 01: BRAIN MRI IMAGES PROCESSING

Processing imaging data is a crucial step, particularly in handling medical images like brain MRI images. Analyzing these images constitutes a key stage in computerized methods, especially in the context of brain image analysis. Our work led to the development of the CE-MRI brain image database, encompassing the axial, sagittal, and coronal planes. Each image presents unique challenges and reveals distinct details. As illustrated in Figure 2, the images displayed therein are susceptible to noise interference. Consequently, there is a requirement for a dependable filter to effectively eliminate this interfering factor. The process for noise suppression is addressed in the subsequent step.

B. STEP 02: ADAPTIVE WIENER FILTERING TO REDUCE NOISE

Adaptive Wiener filtering is the type of signal processing approach that can be used on medical images [30], and we have used Wiener filtering on brain MRI imaging to improve overall image quality by reducing the noise and retaining image detail. The mathematical representation of the adaptive Wiener filter on brain MRI imaging depends on the three parameters, the local window of each pixel of brain MRI images and the noise variance [31]. This is additive noise and the adaptive Wiener filtering works on the local window around each pixel in the image to get a denoised brain MRI image. The step-by-step representation of adaptive Wiener filtering is defined below.

1) The Adaptive Wiener filter operates on a local window around each pixel (x,y) in the image. The filtered output at (x,y) is computed using Equation 1:

$$g(x, y) = w(x, y) * [f(x, y) - m(x, y)] + m(x, y). \tag{1}$$

where $w(x, y)$ is the Wiener filter, $m(x, y)$ is the local mean of the input image in the window around (x,y), and $*$ denotes convolution.

2) The wiener filter is process the images based on the Equation

$$w(x, y) = \frac{[\sigma_f^2(x, y) - \sigma_v^2(x, y)]}{\sigma_f^2(x, y)}. \tag{2}$$

where $\sigma_f^2(x, y)$ is the local variance of the input image in the window around (x,y), and $\sigma_v^2(x, y)$ is the variance of the noise.

The Wiener filter adjusts the strength of the filtering based on the local signal-to-noise ratio (SNR) of the input image. When the SNR is high, the Wiener filter is close to 1, and the filtering is weak, preserving the image features. When the SNR is low, the Wiener filter is close to 0, and the filtering is strong, reducing the noise. Overall, the Adaptive Wiener filter can effectively enhance the quality of brain MRI imaging by removing noise while preserving important image features as shown in the Figure 3.

C. STEP 03: TRAINING OF BRAIN MRI IMAGING BY USING RBF NEURAL NETWORK FILTERING

We employed Radial Basis Function (RBF) neural network filtering as a means to enhance the quality of medical images, particularly those of MRI. RBF neural networks are a type of artificial neural network commonly adopted for image filtering, classification, and pattern recognition tasks. In our study, however, this technique was leveraged to enhance the quality of images and provide pre-classified depictions of brain tumor anomalies [32]. The training of RBF neural network filtering for brain MRI imaging involves the following steps:

1) The first step is data pre-processing and it is an important step to pre-process brain MRI images to remove artifacts as well as noise that can affect the performance of the RBF neural network. This is achieved in the previous steps because we removed noise using adaptive Wiener filtering.
2) The next step is an important step in the functionality of RBF neural networks which is feature extraction.

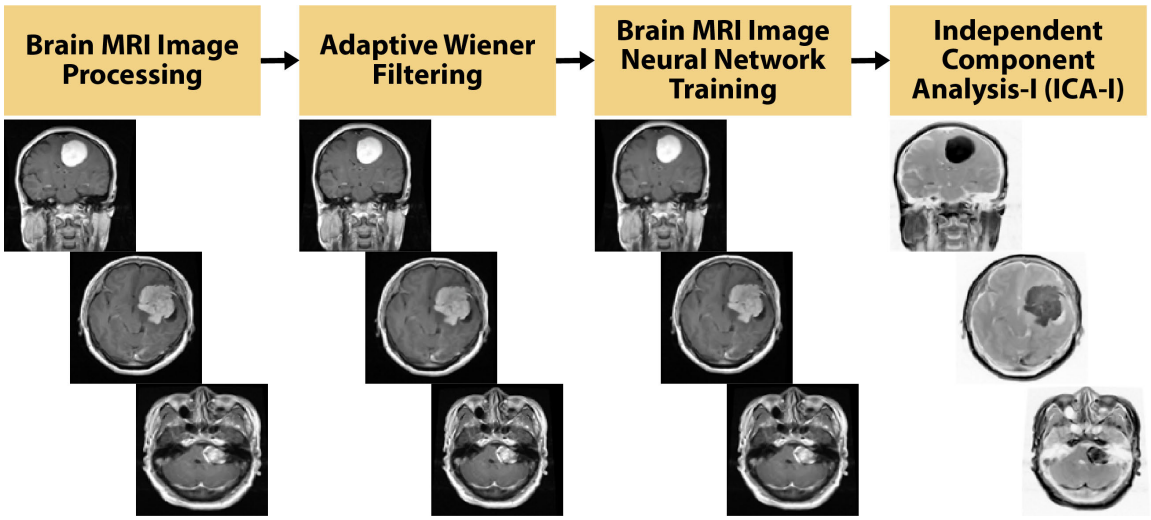

FIGURE 1. The proposed model.

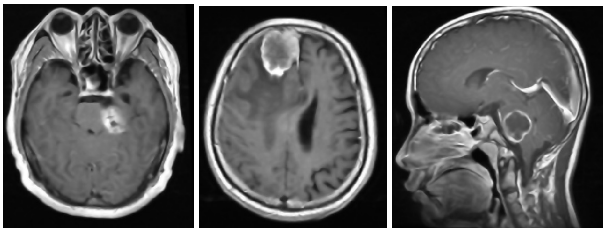

FIGURE 2. Brain MRI images of three planes namely axial plane as shown in Fig(b), sagittal plane as shown in Fig(b) and coronal plane as shown in Fig(c).

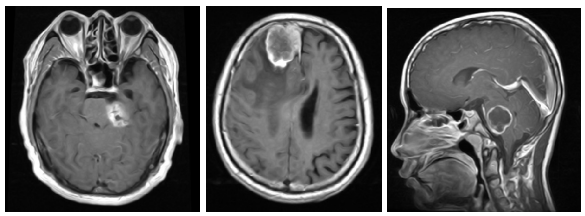

FIGURE 3. Adaptive wiener filtering output of Brain MRI images of three planes axial plane, sagittal plane and coronal plane.

Features are extracted based on the image intensity and spatial information of the data in this proposed method.

3) The RBF neural network is trained based on brain MRI images as well as feature extraction in previous steps. The training image gives corresponding outputs the filtered brain MRI image. The training process is based on learning the mapping of input features to desired output images.
4) After training the brain MRI images, the validation of the RBF neural network is performed and the validation gives the information about the validated data according to the desired output.

The RBF filtering process, as outlined above, is predicated on two parameters. These involve the creation of the image through minimizing its variation and the utilization of RBF to derive a denoised image by reducing the error function on its variation minimization. This methodology serves to lower the noise level and deliver a desirable output image.

1) MINIMIZATION OF THE VARIATION

Variation minimization is mainly used to denoise images and is one of the most effective methods [33], [34]. In this paper, we have used the variation minimization method based on the RBF neural network. The variation minimization variation was introduced by Rudin and Osher [32], and their algorithm is based on the equation 3, which is implemented in this research work for brain MRI images, as well as RBF neural network.

$$f(u) = \int_{\Omega} |D| + \lambda \|\mu_O - \mu\|^2 ddxy. \tag{3}$$

Here, $\int_{\Omega} |D|$ represents the variation model of the image (retinal image or MRI brain image) μ. If the image μ is regular, then Equation 3 becomes simply $\int_{\Omega} |\nabla \mu| dx$. Rudin et al. [32] assumed that noise that corrupts the image can be distinguished from noiseless images based on the size of total variation, which is defined as $\int_{\Omega} \sqrt{\mu_x^2 + \mu_y^2} dxdy$, where Ω represents the image dimensions u_x and u_y with corresponding partial differentiation. The Euler-Lagrange Equation [33] is used to minimize Equation 3, and Equation 4 is obtained.

$$\frac{\partial}{\partial x}\left[\frac{u_x}{\sqrt{\mu^2{}_x + \mu^2{}_y}}\right] + \frac{\partial}{\partial y}\left[\frac{u_y}{\sqrt{\mu^2{}_x + \mu^2{}_y}}\right] - \lambda\,|\mu - \mu_o| = 0. \tag{4}$$

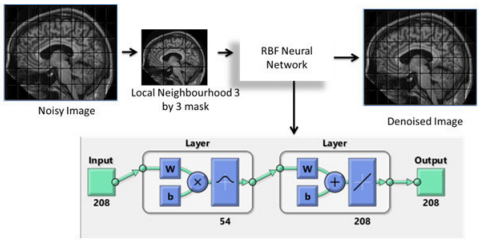

FIGURE 4. RBF Model of Proposed Method for MRI Brain Image.

The Lagrange multiplier, denoted by λ, is given in Equation 5.

$$\lambda = \frac{1}{2\sigma^2}\int \sqrt{{\mu_x}^2 + {\mu^2}_y} - \frac{1}{2\sigma^2}\int \frac{(\mu_o)_x \mu_x}{\sqrt{{\mu_x}^2 + {\mu^2}_y}} + \frac{1}{2\sigma^2}\int \frac{(\mu_o)_y \mu_y}{\sqrt{{\mu_x}^2 + {\mu^2}_y}}. \tag{5}$$

As mentioned earlier, the denoised image is obtained by minimizing the error function, which is represented by Equation 6.

$$E(x,y) = \frac{\partial}{\partial x}\left[\frac{\mu_x}{\sqrt{{\mu_x}^2 + {\mu_y}^2}}\right] + \frac{\partial}{\partial x}\left[\frac{\mu_y}{\sqrt{{\mu_x}^2 + {\mu_y}^2}}\right] - \lambda\left|\mu - \mu_o\right|. \tag{6}$$

Equation 6 represents the main task of obtaining an image where μ is locally constant, with u_x and u_y being the dimensions of the image. To achieve this, it is assumed that $\varepsilon > 0$ and the expression $\sqrt{{\mu^2}_x + {\mu^2}_y + \varepsilon}$ is used.

2) PROPOSED NOISE REDUCTION MODEL USING RBF NEURAL NETWORK

In addition, the denoising of color retinal fundus images and MRI brain images is achieved by minimizing Equation 6 using a proposed RBF neural network. The RBF neural network is composed of three layers: the input layer, the RBF layer, and the output layer. The RBF layer is made up of unity value scalar weights and the input vector, with the entire input vector being fed to each neuron in the RBF network. The output layer consists of a vector of m outputs that are linearly combined to form the output image. The RBF model for MRI brain images is depicted in Figure 4 and mathematically represented in Equation 22.

$$y = f(I) = \sum_{i=1}^{h} h_i I_i(x). \tag{7}$$

The output image, denoted by $f(I)$, is determined by the radial basis function $I(x)$ of the i-th hidden node and the corresponding hidden-to-output weight h_i. The RBF function is based on the distance between the input vector and a predefined vector, which is explained in the previous section and depicted in Figure 4. The total number of hidden nodes is represented by h. This function is mathematically represented by Equation 8.

$$I_i(x) = exp\left[\frac{-\|x - c_i\|}{2{\sigma^2}_i}\right]. \tag{8}$$

The center and spread width of the i-th node are denoted by c_i and σ_i, respectively. All parameters of the RBF neural network are initialized before training. The weight can be initialized with small random values or zero, and the spread initial value can be selected as the average of the nearest neighbour distances among the initial centers. After training, the RBF image can be represented by the equation given below as Equation 9

$$\mu = N(\mu_o, h_i, c_i). \tag{9}$$

The noisy image is denoted by μ. The gray level output of each pixel can be calculated using Equation 10 as $\mu_O(x,y)$.

$$N(x,y) = \left(\sum_{i=1}^{h} h_i \exp\left[\frac{-\|M_o(x,y) - c\|_i}{2{\sigma^2}_i}\right]\right). \tag{10}$$

$M_o(x,y)$ represents the grey level values of the neighboring pixels corresponding to the pixel values of $\mu_O(x,y)$. The window size of the pixels can be 3 by 3, 5 by 5, etc. and it is illustrated in Figure 4.

3) TRAINING OF RBF NEURAL NETWORK IMAGE

The aim is to minimize the error during the training of the image $M_o(x,y)$ using the RBF neural network. The network is trained for a maximum number of iterations until the error is less than the convergence error threshold. The parameters for the RBF neural network are determined using Equation 11, while the training parameters are dependent on Equation 12.

$$h_i(s+1) = h_i(s) - \eta_1 \Delta h_i(s). \tag{11}$$

$$c_i(s+1) = c_i(s) - \eta_2 \Delta c_i(s). \tag{12}$$

The RBF neural network parameters, such as weights and centers, are updated at each iteration using the update rules given in Equation 13, where $h_i(s+1)$ and $c_i(s+1)$ represent the updated values of the parameters at the next iteration, while $h_i(s)$ and $c_i(s)$ are the current values, and η_1 and η_2 are positive learning rates. The update is performed by minimizing the error function of Equation 6 to obtain the parameter variations Δh_i and Δc_i

$$\Delta h_i = \sum_{x,y} \frac{\partial E(x,y)}{\partial h_i}. \tag{13}$$

$$\Delta c_i = \sum_{x,y} \frac{\partial E(x,y)}{\partial c_i}. \tag{14}$$

$$\frac{\partial E(x,y)}{\partial h_i} = \frac{\frac{\partial}{\partial x}\left[\frac{u_x}{\sqrt{{\mu^2}_x + {\mu^2}_y}}\right]}{\partial h_i} + \frac{\frac{\partial}{\partial y}\left[\frac{u_y}{\sqrt{{\mu^2}_x + {\mu^2}_y}}\right]}{\partial h_i}$$

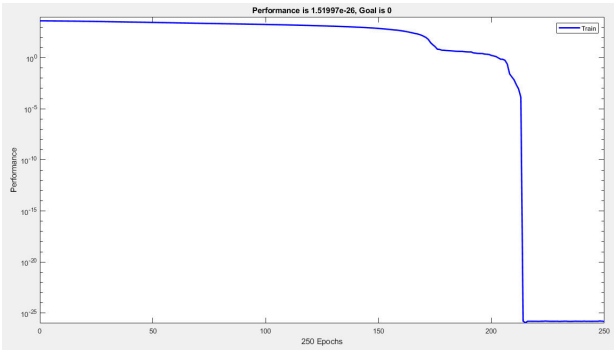

FIGURE 5. Illustration of training of rbf neural network for brain MRI images.

$$-\frac{\partial\lambda}{\partial h_i}(\mu-\mu_o)-\lambda\frac{\partial\mu}{\partial h_i}. \tag{15}$$

$$\frac{\partial E(x,y)}{\partial c_i}=\frac{\frac{\partial}{\partial x}\left[\frac{u_x}{\sqrt{\mu^2{}_x+\mu^2{}_y}}\right]}{\partial c_i}+\frac{\frac{\partial}{\partial y}\left[\frac{u_y}{\sqrt{\mu^2{}_x+\mu^2{}_y}}\right]}{\partial c_i}-\frac{\partial\lambda}{\partial c_i}(\mu-\mu_o)-\lambda\frac{\partial\mu}{\partial c_i}. \tag{16}$$

The process of training is essential to achieve the desired outcome of the image. For instance, in order to denoise brain MRI images, training is conducted and the results are presented in Figure 5.

D. STEP 04:INDEPENDENT COMPONENT ANALYSIS FOR BRAIN MRI IMAGES

In the methodology section, we elaborate on our utilization of Independent Component Analysis (ICA) as the computational technique chosen to disentangle intricate, multivariate signals into self-standing, non-Gaussian components. Our primary application of ICA is within the realm of brain MRI image analysis, where it serves the purpose of distinguishing and isolating the autonomous components residing within these MRI images. Consequently, the outcome comprises a collection of normalized images that conspicuously exhibit the extracted independent component brain MRI images, characterized by their normalized and coherent contrast. Equation 17 demonstrates how the Independent Component Analysis (ICA) approach can be further developed from its mixed model. The equation illustrates that the observed mixed signals (X) can be decomposed into a matrix of independent source signals (S) that are linearly combined through a mixing matrix (A). By utilizing this equation, ICA can effectively separate and extract the independent source signals from the observed mixed signals.

$$X=AS. \tag{17}$$

The ICA model is represented by Equation 17. It assumes that the mixture vector X and independent component vector S are random vectors with zero mean and unit variance. The unknown matrix A is the mixing matrix of the independent components, assumed to be in a square pattern. Additionally, the ICA model assumes that the independent component vector S has a non-Gaussian distribution. The estimation of non-Gaussianity is a crucial parameter in the ICA model, as it is required for the calculation of independent components. The analysis is based on the random vector X, and the main goal is to estimate the unknown components A and S using X. If the unknown mixing matrix A can be estimated, its inverse can be computed as W, which enables the calculation of the independent component vector S. This process is expressed as follows:

$$S=A^{-1}X=WX. \tag{18}$$

To estimate W, the FASTICA algorithm [35] can be utilized, which initializes random vectors and utilizes a fixed point algorithm to obtain a single independent component. For multiple independent components, the FASTICA algorithm must be iterated n times with weight vectors $w_1, w_2, w_3 \ldots\ldots\ldots w_n$. However, there is a high probability of correlation between the vector values, which may result in different random vectors converging at the same maxima. To prevent this, it is crucial to de-correlate or orthogonalize the weight vector outputs $w_1^TX, w_2^TX, w_3^TX \ldots..w_n^TX$ using the Gram-Schmidt-Orthogonalization method [36] after each iteration.

ICA comprises two architectures designed for deriving feature vectors. The chosen architecture, ICA1, is specifically applied to identify components in medical images, particularly in the context of brain MRI images. Its implementation involves evaluating ICA's effectiveness in contrast enhancement. Notably, ICA1 demonstrates excellent contrast image quality and performs well in segmenting abnormal regions, such as brain tumors. The following section offers a detailed explanation of the application of ICA1 on brain MRI images, elaborating on its capabilities in enhancing contrast and accurately delineating abnormal regions within the images.

1) ICA ARCHITECTURE 1 (ICA1) ON BRAIN MRI IMAGES

The ICA1 model involves preparing the image database in a matrix format, where each row vector corresponds to an individual image or ICA independent component. This model is illustrated in Fig. 6, where images are regarded as random variables and pixels are treated as trials. As depicted in the figure, the data matrix X, also known as the mixture matrix, is a combination of n independent ICA components or images. The coefficient matrix, denoted by W, is calculated using the FASTICA algorithm, with W being required to be in a square pattern. The source matrix, denoted by S, comprises n independent basis images. In the ICA1 approach, the data matrix has n training samples with image column vectors of length m. The dimension of the data matrix is represented as $m \times n$ with column data matrix $X = x_1, x_2, \ldots, x_n$. The

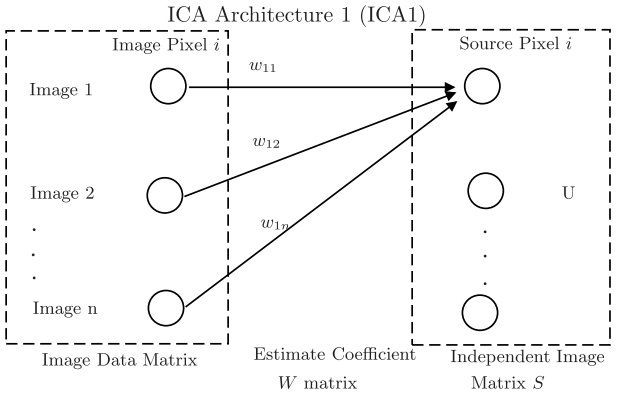

FIGURE 6. ICA Architecture 1 model.

main idea behind implementing ICA1 is to transpose the data matrix X into a mixture row data matrix $Y = X^T$. The Y matrix is represented as $Y = y_1, y_2, \ldots\ldots y_m$. The following steps are followed to implement ICA1.

a: CENTERING PROCESS

In the first step, the mean vector is estimated from the data matrix as $\mu I = \frac{1}{m}\sum j = 1^m y_j$. This mean vector is subtracted from each column vector of the data matrix such that $(y_j - \mu_I) \rightarrow \overline{y_j} \rightarrow \overline{y_v}$. Here, $\overline{y_v}$ represents the vertically centered row data matrix, and each column vector of the data matrix has been subtracted by the mean vector to generate a zero-mean image row data matrix.

b: WHITENING PROCESS

The subsequent step involves the whitening of the vertically centered data matrix using Principal Component Analysis (PCA). To perform this, orthonormal eigenvectors $V = v_1, v_2, v_3 \ldots..v_n$ of the covariance matrix $\sum_I = \frac{1}{m}\sum_{j=1}^{m} y_j y_j^T$ are computed, with the largest positive eigenvalues (p) as $y_1 \geq y_2 \geq \ldots\ldots.. \geq y_p$. The whitening process can be expressed mathematically as:

$$H = VD^{-\frac{1}{2}}. \tag{19}$$

where D is the diagonal matrix of the largest eigenvalues.

c: TRANSFORMATION PROCESS

After performing the whitening process, the centered row data matrix $\overline{y_v}$ is transformed using the orthonormal eigenvectors V as follows:

$$\widetilde{y} = H^T \overline{y_v}. \tag{20}$$

These pre-processing steps play a crucial role in the application of ICA, as they prepare the data matrix for the subsequent analysis. Once these steps are performed, ICA is applied to the whitened data matrix, denoted by H, to obtain a matrix S_I consisting of independent images arranged row-wise. This is achieved by multiplying the whitened data matrix $\widetilde{y}$ with a coefficient matrix W_I, where the row vectors of S_I correspond to the base images of ICA1. The final independent images are obtained by projecting the vertically centered data matrix on the independent eigenvectors of the base images, as given by $Z = \overline{y_v}\widetilde{y}^T W_I$. The number of independent components in Z depends on the user's requirements. In the case of brain MRI images, which are in JPEG format and contain three independent components, ICA1 yields three independent components. This process is explained in greater detail below.

The utilization of Independent Component Analysis (ICA) is a crucial step in our approach, wherein we apply ICA individually to each component of the brain MRI images generated by the RBF neural network. This process requires a deep comprehension of the intrinsic imaging and biological characteristics of these images before any normalization steps are taken. It's noteworthy that the three components of the brain MRI images are linearly independent. However, a closer examination reveals distinct attributes: the first component (ICA1) contains both significant luminance information and noise, the second component exhibits reduced noise, while the third component introduces shadows and additional noise. The primary objective of our study centers on identifying a suitable component within the brain MRI images that showcases well-contrasted regions against a more uniform background. Consequently, we employ ICA on each non-uniform background output image to enhance the contrast levels in various regions of the contrast-enhanced MRI (CE-MRI) brain images when juxtaposed against their respective backgrounds. It's essential to bear in mind that the CE-MRI database encompasses three distinct imaging planes, each offering unique information. Furthermore, tumors may manifest in various locations within each imaging plane.

ICA1 architecture is employed to investigate its efficacy in enhancing the contrast of various brain MRI regions. The findings of this study are displayed in Fig. 7, which demonstrates that the second component of ICA1 (basis on measurement of contrast and signal to noise ratio also) produced superior results in terms of improving the contrast of different regions against their background compared to the first and third components. The primary contribution of this research is the validation and implementation of ICA1 architecture to produce a normalised and enhanced contrast brain MRI image, taking into account imaging properties such as biological, structural, and imaging properties. This implementation could aid in accurately segmenting brain tumors.

IV. POST-PROCESSING:BRAIN TUMOR CLASSIFICATION

Our proposed method focuses on the impact of enhancement techniques based on ICA1 analysis on the classification process. The postprocessing step involves classifying brain tumors using Support Vector Machine (SVM), a supervised learning method that utilizes statistical learning theory to classify data [37]. The first essential step in this process is data labeling, which entails representing the training dataset

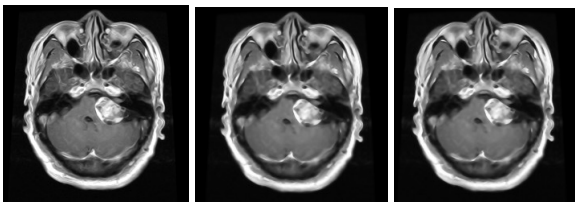

FIGURE 7. Comparsion of Enhancement techniques with ICA1 enhanced image. Fig(a) is first component of ICA1. Fig(b) is second component of ICA1 Fig (c) is third component of ICA1.

as $D = \{|x, y|, |x \rightarrow datasample, y \rightarrow classlabel|\}$. SVM's primary objective is to calculate functions represented by f, such as $f(x) = y$, for all image data or pixels to achieve accurate brain tumor classification. The mapping function's primary goal is to establish a relationship between the labeled samples and classified data, enabling accurate brain tumor detection. The decision function is utilized to classify the tumor and non-tumor regions, and its mathematical representation is known as the feed-forward process of SVM classification, as illustrated below:

$$D(m) = \left(\sum_{i=1}^{N} \alpha_i y_i K(d_i m_i) + t \right). \tag{21}$$

The equation shown in 21 represents the alpha coefficient (α_i) of support vector class labels or feature vectors. The SVM vector is denoted as y_i, and the input vector is denoted as d_i. The kernel function with a bias t is represented by $K(d_i m_i)$. In SVM-based brain tumor image classification, the process can be broken down into three steps. The first step involves selecting the feature vector through feature vector extraction. The second step involves training the data, and the third step involves tumor classification and identification of the tumor region.

The feature vector is created by combining data in an array, allowing for object classification on a per-feature vector basis. In brain tumor images, the image is first converted to a binary image, as seen in Figure 8(b), and then skeletonized, as shown in Figure 8(a). The image is then divided into zones and appended areas to form the image matrix. The generated feature is based on Euler numbers and related parameters, such as pixel distributions with the x and y planes. Approximately 100 feature vectors are generated to classify the tumor region in the image. For our research, we processed 310 brain tumor images, and SVM training was conducted by combining the feature vectors in matrix form to classify tumor regions. The support vectors of the SVM method are the closest collection of data points to the decision surface, making it challenging to classify brain tumors. These points are determined based on a location optimization process to decide the surface to locate the anomalous region. SVM maximizes the margin around the hyperplane separation, and the decision function is based on the training sample subset to identify the tumor region. The output of the SVM process is presented in Figure 8.

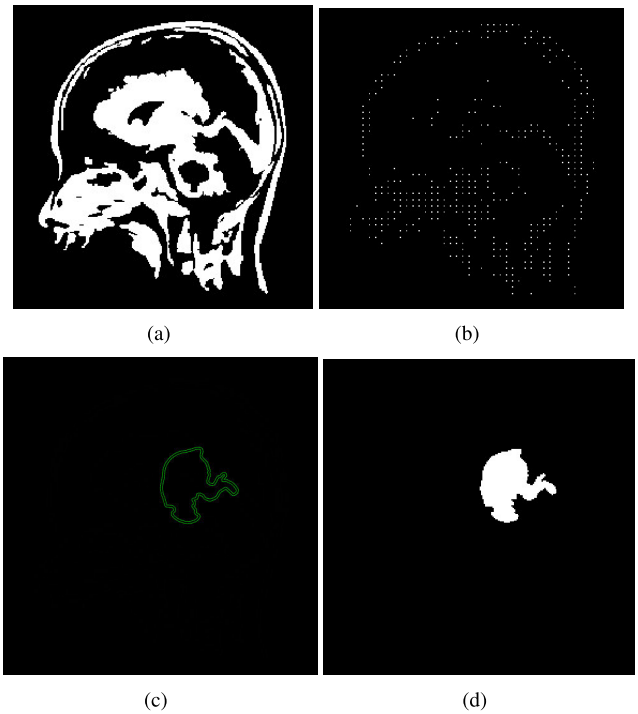

FIGURE 8. Figure shows the steps involved in the SVM-based classification process for detecting brain tumors. In Figure (a), the original brain image is converted to a binary image. Next, in Figure (b), the binary image is skeletonized. The resulting image is then divided into zones and appended areas to form an image matrix. The generated feature vector is based on Euler numbers and related parameters, such as pixel distributions with *x* and *y* planes, resulting in about 100 feature vectors for each image. The SVM classifier is then trained using these feature vectors in matrix form, as shown in Figure(c), to classify tumor regions. Finally, the decision function of the SVM is used to detect the tumor region, as shown in Figure(d).

V. DATABASE AND PARAMETERS MEASUREMENT

he efficacy of the suggested method is assessed through three distinct criteria: the enhancement of the brain image, the segmentation of the tumor region, and the classification of brain tumors. The enhancement outcomes are evaluated based on two factors: contrast and peak signal-to-noise ratio. The segmentation outcomes are appraised using five metrics: mean, standard deviation, entropy, kurtosis, and skewness. The performance of the brain tumor classification is determined using sensitivity, specificity, and accuracy measures.

A. MEASURING PARAMETERS: ENHANCEMENT OF THE BRAIN IMAGE

The enhancement results are assessed for performance by quantifying five parameters: peak signal-to-noise ratio and contrast. Each of these parameters is further explained below.

1) SIGNAL TO NOISE RATIO OF THE BRAIN MRI IMAGE

The Peak Signal to Noise Ratio (PSNR) is a parameter used to assess the quality of a brain image compared to a noisy image. It calculates the ratio between the maximum possible signal level and the noise level present in the MRI image of

the brain. The PSNR calculation formula, as introduced by L. Jong and Sen in 1980, is represented by the Equation 22.

$$PSNR = 20log_{10}\left(\frac{R}{\sigma}\right). \tag{22}$$

In this equation, the value of the PSNR is obtained by taking the logarithm in base 10 of the ratio between the maximum value of the signal R and the standard deviation of the noise σ. The standard deviation σ represents the variability of the image intensities produced by the noise. A higher value of σ represents more noise in the image, while a lower value represents less noise. The maximum image value (R) related to the highest possible intensity level that can be represented in the image. It typically ranges from 0 to 255 in an 8-bit grayscale image, where 0 represents black and 255 represents white.

2) IMAGE CONTRAST

From the perspective of brain MRI images, image contrast (IC) suggests the difference in intensity level between a particular pixel and its surrounding neighboring pixels in the image. Mathematically, image contrast (IC) can be represented by:

$$Contrast = \sum_{i=0}^{m-1}\sum_{j=0}^{n-1}(i-j)^{2} f\,(i,j)\,. \tag{23}$$

B. MEASURING PARAMETERS: SEGMENTATION OF BRAIN TUMOR

The segmentation results are assessed for performance by quantifying five parameters: mean, standard deviation, entropy, kurtosis, and skewness. Each of these parameters is further explained below.

1) MEAN

The average parameter is calculated by multiplying the pixel values of the image by the total number of pixels in the image. The calculation of the average is represented by the following equation:

$$Mean = \left(\frac{1}{m \times n}\right)\sum_{i=0}^{m-1}\sum_{j=0}^{n-1} I(i,j). \tag{24}$$

where 'm' and 'n' represent the number of pixels corresponding to the dimensions of the image.

2) STANDARD DEVIATION

The standard deviation (STD) is obtained by taking the square root of the variance or the central mean of the image. It gives insight into how pixels are distributed relative to the average and reveals information about non-uniformity in the image. A higher average value suggests greater saturation and increased contrast at the edges of the image. Mathematically, this can be represented in the equation 25.

$$STD(\sigma) = \sqrt{\left(\frac{1}{m \times n}\right)\sum_{i=0}^{m-1}\sum_{j=0}^{n-1}(I\,(i,j) - M)^2}. \tag{25}$$

3) ENTROPY

Entropy is a metric that quantifies the level of randomness or unpredictability in an image's texture. It provides a measure of the amount of information needed to describe the distribution of pixel intensities in the image. Higher entropy values indicate a more complex and diverse texture, while lower entropy values indicate a more regular and uniform texture. Mathematically, entropy can be represented in the Equation 26.

$$Entropy = -\sum_{i=0}^{m-1}\sum_{j=0}^{n-1} f\,(i,j)\log_2(i,j)\,. \tag{26}$$

4) KURTOSIS

In the context of brain MRI images, kurtosis is a parameter that provides insight into the probability distribution of random variables in the image. This helps us understand the shape of the distribution and the presence of outliers or outliers. The kurtosis is denoted Kurt(I) for image I, indicating that it applies specifically to the features of that particular image. Mathematically, kurtosis can be represented using Equation 27:

$$kurt\,(I) = \left(\frac{1}{m \times n}\right)\frac{\sum((f(i,j) - M)^4)}{STD^4}. \tag{27}$$

By calculating the kurtosis of brain MRI images, we can better understand the distribution of intensities, which can be useful in tasks such as identifying abnormalities, detecting subtle changes, or characterizing specific tissue properties. It helps in understanding the statistical properties of image data and can help in various medical image analysis applications.

C. SKEWNESS

In the context of brain MRI images, skewness is a parameter that provides information about the similarity or dissimilarity of pixel distributions in the image. Skewness measures the asymmetry of the distribution and helps us understand whether pixel values are more concentrated on one side or the other.

$$\mathrm{SK}\,(I) = \left(\frac{1}{m \times n}\right)\frac{\sum(f\,(i,j) - M)^3}{STD^3}. \tag{28}$$

By calculating the asymmetry of brain MRI images, we can assess the symmetry or asymmetry of the pixel distribution, which can be useful in various applications such as tissue characterization, lesion detection and abnormality identification. Skewness helps us understand the statistical properties of image data and can aid in the analysis and interpretation of brain MRI images.

D. MEASURING PARAMETERS: CLASSIFICATION OF BRAIN TUMOR

To assess the effectiveness of classification, we used a combination of training and test data. To ensure a comprehensive evaluation of the database, we used cross-validation, a widely adopted technique for validating the performance of classification models. The evaluation of the classification model involved the use of the following parameters.

1) SENSITIVITY

In the context of brain MRI, sensitivity refers to the measurement of precisely identified pixels belonging to positive classes. It quantifies the ability of a classification model to correctly detect positive instances. Mathematically, sensitivity is calculated as the ratio of the total number of true positive pixels to the total number of pixels identified as positive, as defined in the equation 29. Sensitivity is also commonly referred to as True Positive Rate (TPR). The equation 29 represents the sensitivity calculation:

$$\text{Sensitivity} = \frac{\text{TP}}{\text{TP} + \text{FN}} \tag{29}$$

where as: TP refers to the number of true positive pixels, indicating the number of correctly identified pixels belonging to the positive class. FN represents the number of false negative pixels, indicating the number of pixels belonging to the positive class that were incorrectly identified as negative.

2) SPECIFICITY

In the context of brain MRI images, specificity refers to the measurement of precisely identified pixels belonging to negative proportions or classes. It quantifies the ability of a classification model to correctly detect negative instances. Mathematically, specificity is calculated as the ratio of the total number of true negative pixels to the total number of pixels identified as negative, as defined in the equation 30. Specificity is also commonly referred to as true negative rate (TNR). The equation 30 represents the specificity calculation:

$$\text{Specificity} = \frac{\text{TN}}{\text{TN} + \text{FP}} \tag{30}$$

where as: TN refers to the number of true negative pixels, indicating the number of correctly identified pixels belonging to the negative class. FP represents the number of false positive pixels, indicating the number of pixels belonging to the negative class that were incorrectly identified as positive.

3) ACCURACY

In the context of brain MRI, accuracy is a parameter that provides information about the accuracy of predictions regarding true pixels. The most effective approach to evaluating the performance of a model's predictions is to count the number of pixels detected accurately. Accuracy measures the proportion of correct predictions of true pixels and is mathematically defined as equation 31.

$$Accuracy(AC) = \frac{TP + TN}{TP + FP + TN + FN}. \tag{31}$$

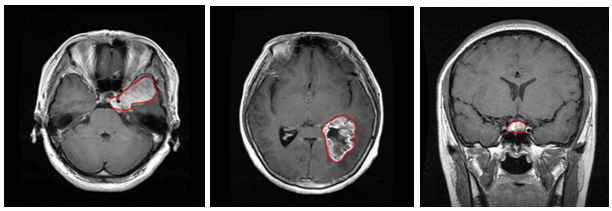

(a) (b) (c)

FIGURE 9. CE-MRI images illustrate different types of brain tumors as follows: Figure (a) depicts a meningioma brain tumor. Figure (b) shows a glioma brain tumor. Figure (c) shows a pituitary brain tumor.

4) DICE SCORE

In the context of brain MRI, the Dice Score (DSC) is a parameter that provides information about the overlap ratio between the predicted output and the actual ground truth values. It quantifies the similarity between predicted and ground truth regions of interest. The Dice score is normalized by considering the true positive values compared to the mean of the predicted and ground truth values. Mathematically, the Dice score is represented as equation 32.

$$DSC = \frac{2 \times TP}{(2 \times TP + FN + FP)} \tag{32}$$

By evaluating the Dice score in brain MRI, we can assess the degree of overlap and similarity between the predicted output and the ground truth values. The Dice score provides a valuable measure of model performance and helps assess the accuracy and quality of segmentation or registration tasks in MRI analysis of the brain

E. DATABASES

We are making use of the Contrast-Enhanced Magnetic Resonance Imaging (CE-MRI) image dataset, which was established by Nanfang Hospital in Guangzhou, China, and the General Hospital at Tianjin Medical University, China, during the period spanning from 2005 to 2010. The term "CE-MRI brain dataset" typically refers to a compilation of images generated through contrast-enhanced magnetic resonance imaging techniques, which are crucial for examining biological structures. In CE-MRI procedures, contrast agents are introduced during scans to enhance the visibility of specific tissues or detect abnormal conditions within MRI brain images. This dataset comprises 3064 images collected from 233 individuals, including 930 pituitary tumors, 708 meningiomas, and 1426 gliomas. These images have a resolution of 512 by 512 pixels, with each pixel measuring $0.49 \times 0.49, \text{mm}^2$, and a $1mm$ gap between slices. The identification of tumors within these images was performed manually by three highly skilled radiologists. Figure 9 showcases several examples from this CE-MRI image dataset.

Key considerations regarding CE-MRI datasets and their applications encompass:

1) Different imaging techniques, including contrast-enhanced T1-weighted sequences, are utilized to

TABLE 1. Impact of image enhancement technique on ce-mri image.

	Without Image Enhancement Technique		With Image Enhancement	
Database:Images Types/Parameters	PSNR	Contrast	PSNR	Contrast
Meningiomas Tumor Images	19.91	38.12	**23.93**	**74.89**
Gliomas Tumor Images	19.98	28.98	**24.99**	**71.22**
Pituitary Tumor Image	21.25	42.02	**25.46**	**79.98**

TABLE 2. The analysis of the performance of different image enhancement methods.

	HE		CLAHE		BBHE		Proposed Method	
Database:Images Types	PSNR	Contrast	PSNR	Contrast	PSNR	Contrast	PSNR	Contrast
Meningiomas Tumor Images	19.12	39.30	21.22	40.98	20.01	38.12	**23.93**	**74.89**
Gliomas Tumor Images	20.34	27.21	20.97	29.01	19.94	28.98	**24.99**	**71.22**
Pituitary Tumor Image	18.95	41.01	22.01	42.97	21.05	42.02	**25.46**	**79.98**

acquire CE-MRI datasets. These enhanced T1-weighted sequences facilitate the observation and quantification of the distribution of contrast agents within tissues.

2) CE-MRI datasets are frequently compiled for research objectives as part of clinical studies. Notably, public repositories and research institutions like The Cancer Imaging Archive (TCIA) and the Alzheimer's Disease Neuroimaging Initiative (ADNI) maintain MRI databases that encompass CE-MRI data, in addition to other imaging modalities.
3) CE-MRI datasets typically comprise 3D volumetric image sequences obtained at various time intervals following the injection of a contrast agent. These datasets may encompass baseline anatomical sequences, supplementary pre-contrast images, and dynamic post-contrast series.
4) CE-MRI assesses brain tumors and defines their boundaries in brain tumor imaging. Contrast-enhanced sequences are instrumental in pinpointing tumor-afflicted areas within MRI brain images, thereby assisting in diagnosis, treatment strategy formulation, and therapy effectiveness evaluation.
5) The provided dataset contains 3064 contrast-enhanced T1-weighted images collected from 233 individuals, encompassing three distinct categories of brain cancers: meningiomas (comprising 708 slices), gliomas (comprising 1426 slices), and pituitary tumors (comprising 930 slices) [38]. In our approach, we allocated 70% of the images for the training phase, which includes preprocessing steps such as brain image processing and enhancement (ICA-1). The remaining 30% of the dataset contains testing the classifier, which involves post-processing modules utilizing an SVM-based classifier. It is important to note that images from the same subjects of each brain tumor type are included in both the training and testing process of the method.

VI. RESULTS AND DISCUSSION

A. ANALYSIS ON ENHANCEMENT TECHNIQUE ON BRAIN MRI IMAGES

The Results and Discussion section of the research paper presents an analysis of peak signal-to-noise ratio (PSNR) and contrast in brain MRI images. This section provides a detailed review of PSNR values and contrast analysis based on CE-MRI image database and analysis is given below.

1) IMPACT OF ENHANCEMENT TECHNIQUE

The results of the analysis of our proposed method on the CE-MRI image database, with and without the use of enhancement techniques, are presented in table 1. The table shows the results obtained by applying our method to different types of brain MRI images in the CE-MRI image database, in particular the Meningiomas Tumor Images, Gliomas Tumor Images and Pituitary Tumor Image. After careful analysis, he validated that our method significantly improves the contrast of every type of brain MRI image in the CE-MRI image database. The contrast enhancement amounts to 40 indicating a substantial improvement in the visibility and distinction of various structures or regions in the images as well as leading to accurate segmentation and classification of brain tumors. Additionally, the analysis reveals a 3dB improvement in the peak signal-to-noise ratio (PSNR) metric, signifying the improved quality and fidelity of the processed images. These improvements validate the capability of our proposed technique for the analysis of medical images, not only limited to brain abnormalities observed in the CE-MRI image database, but also extendable to other types of medical images. For example, our method has potential applicability to retinal fundus images, allowing better analysis of eye abnormalities. Therefore, the results highlight the efficiency and versatility of our technique in improving and analyzing medical images, especially in the context of brain abnormalities in the CE-MRI brain MRI database.

TABLE 3. Performance analysis of segmentation model of brain tumor.

Image Types	Mean	STD	Entropy	Kurtosis	Skewness
Meningiomas Tumor Images	0.0051	0.100	3.38	36.32	5.96
Gliomas Tumor Images	0.0050	0.099	3.13	34.23	5.87
Pituitary Tumor Image	0.0052	0.098	3.11	33.12	5.81

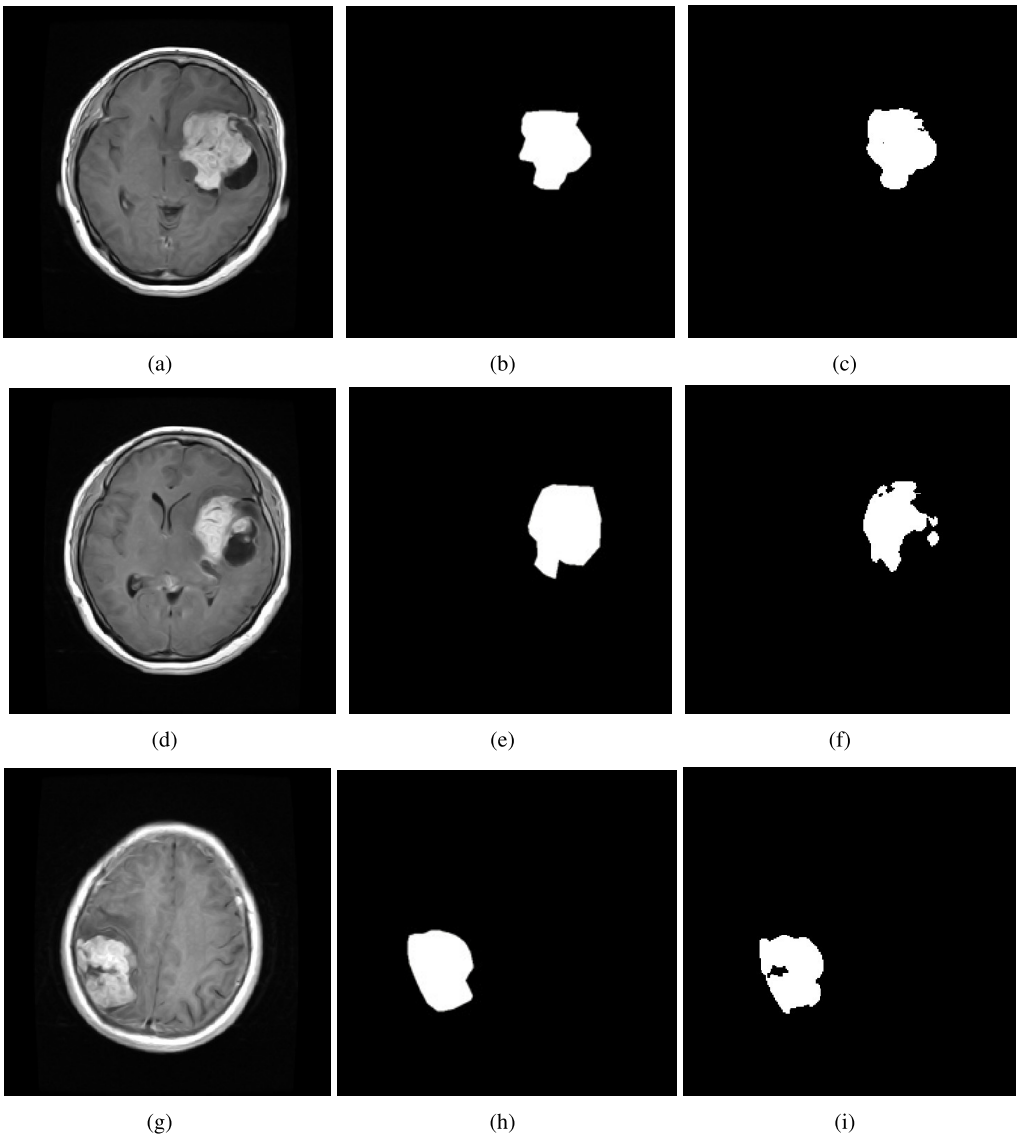

FIGURE 10. Brain tumor segmentation results of the proposed method of different position of Axial plane Brain MRI Image. The first column represents the original images of the database. The second column represents the ground truth and third column represents the output of the image.

B. COMPARATIVES ANALYSIS OF IMAGE ENHANCEMENT WITH EXISTING IMAGE ENHANCEMENT TECHNIQUES

The different image enhancement techniques: Histogram Equalization (HE), Contrast Limiting Adaptive Histogram Equalization (CLAHE), Brightness Bi-Histogram Equalization (BBHE) are compared to our proposed method. By analyzing the performance of different image enhancement techniques, it can be observed that the proposed methods consistently outperform other techniques in terms of PSNR and contrast. The proposed method achieves the highest PSNR and contrast values for each type of Brain MR image, indicating superior enhancement and better visibility of structures in brain MRI images. This comparative analysis highlights the effectiveness of the proposed method in improving image quality, especially in terms of PSNR and Contrast. This implies that the proposed method has the

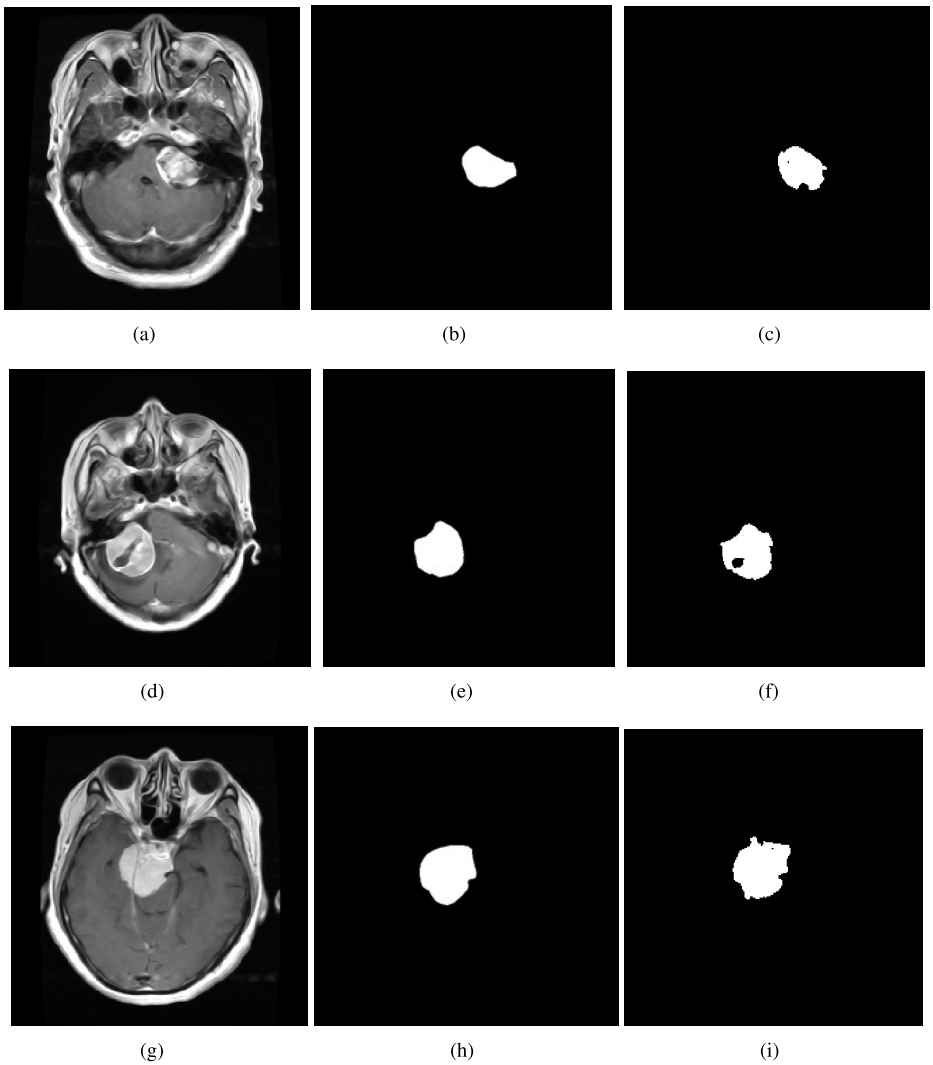

FIGURE 11. Brain tumor segmentation results of the proposed method of different position of Coronal plane Brain MRI Image. The first column represents the original images of the database. The second column represents the ground truth and third column represents the output of the image.

TABLE 4. Comparison of performance segmentation model of brain tumor detection.

Method	Classifier	Mean	STD	IC	PSNR(dB)
Vrooman et al. [39]	K-NN	0.0032	0.071	0.19	0.75
Logeswari et al [40]	SOM	0.0028	0.067	0.18	0.76
Kharrat et al.[41]	GA	0.0033	0.074	0.21	0.78
Mamta et al.[18]	GCNN	0.0034	0.077	0.23	0.79
Mandle et al.[42]	Kernel-Based SVM	0.0031	0.072	0.22	0.98
Proposed Method	ICA-NN-SVM	0.0051	0.099	0.753	2.9

potential to contribute significantly to the analysis of medical images, especially those related to brain abnormalities in the CE-MRI image database.

C. ANALYSIS OF SEGMENTATION MODULE PERFORMANCE

The performance of the brain tumor segmentation method on the CE-MRI database is analyzed by analyzing different parameters. These parameters are analyzed to assess the effectiveness of the method in the precise identification and delineation of brain tumors. Statistical measures, as presented in the table 3, are used to analyze the performance of the proposed method. These parameters provide valuable information about the quality of the segmentation by highlighting the contrast obtained in the brain region and the normalization of the image, which facilitates an accurate

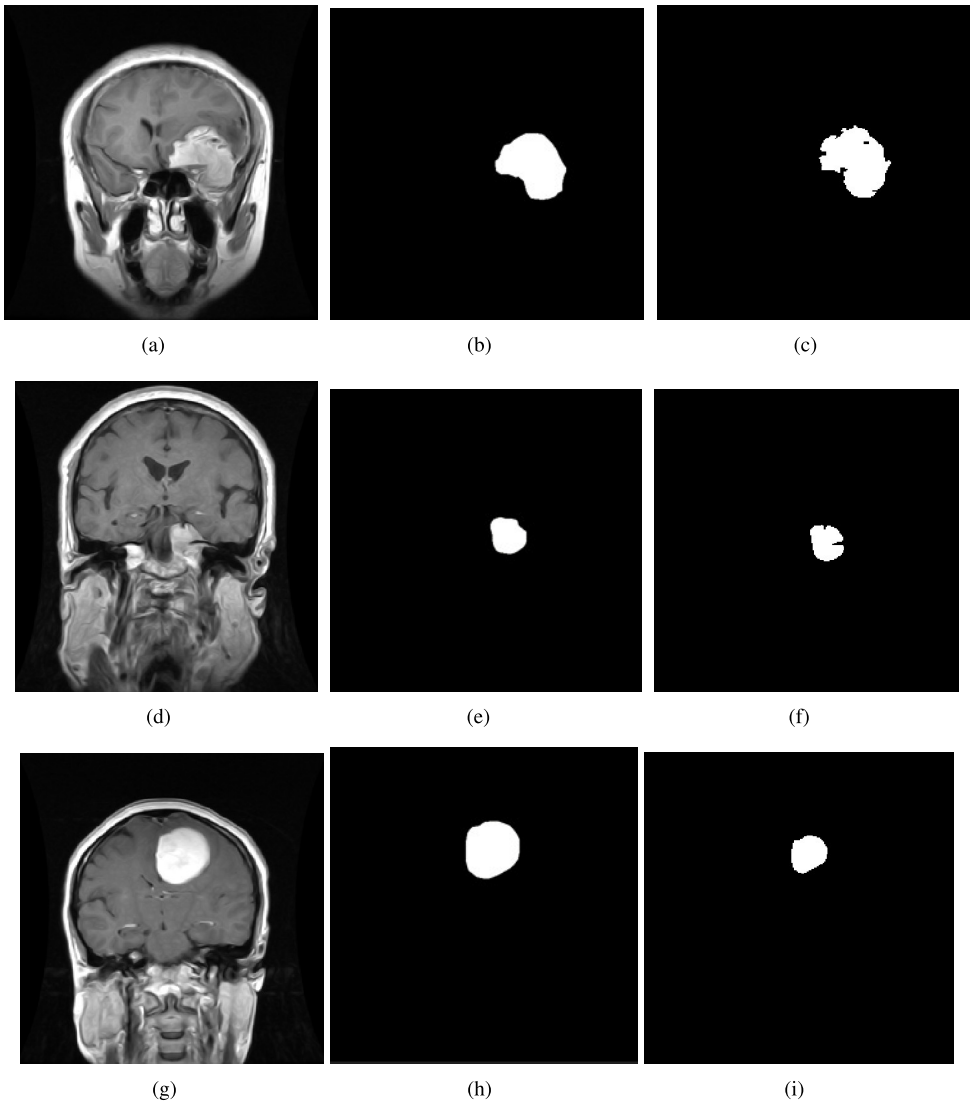

FIGURE 12. Brain tumor segmentation results of the proposed method of different position of Sagittal plane Brain MRI Image. The first column represents the original images of the database. The second column represents the ground truth and third column represents the output of the image.

TABLE 5. Impact of image enhancement technique on classification model.

	Without Image Enhancement Technique				With Image Enhancement			
Database:Images Types/Parameters	Sen	Spec	Acc	DSC	Sen	Spec	Acc	DSC
Meningiomas Tumor Images	0.67	0.66	0.66	0.64	0.99	0.99	0.99	0.97
Gliomas Tumor Images	0.62	0.61	0.61	0.61	0.98	0.99	0.99	0.96
Pituitary Tumor Image	0.67	0.66	0.66	0.66	0.99	0.98	0.98	0.96
Overall Performance	0.65	0.64	0.64	0.63	0.99	0.99	0.989	0.981

segmentation of the tumor. The table 3 shows the capability of the proposed methods as it leads to an accurate segmentation of the brain tumor and visualizes the analysis is shown in Figure 10, Figure 11 and Figure 12. Visualizations of tumor detections clearly show the module's ability to accurately identify and locate brain tumors. These results underscore the competence of the module and its potential to aid in brain tumor detection, providing valuable evidence of its capabilities in the field.

D. COMPARISON OF SEGMENTATION MODULE PERFORMANCE BASED ON DIFFERENT CLASSIFIER

The Mnay researchers used different classifiers to segment the brain tumors and analyze the corresponding images

TABLE 6. Comparison of performance classification model of brain tumor detection with different classifier.

method	Sensitivity	Specificity	Accuracy	DSC	Time
K-NN [39]	0.39	0.42	0.85	0.81	3.7s
SOM [40]	0.43	0.52	0.92	0.83	4.8s
GA [41]	0.51	0.54	0.98	0.85	2.8s
GCNN [18]	0.85	0.89	0.96	0.89	0.92s
Kernel-Based SVM [42]	0.98	0.98	0.98	0.94	0.83s
Proposed Method	0.99	0.99	0.989	0.981	0.43s

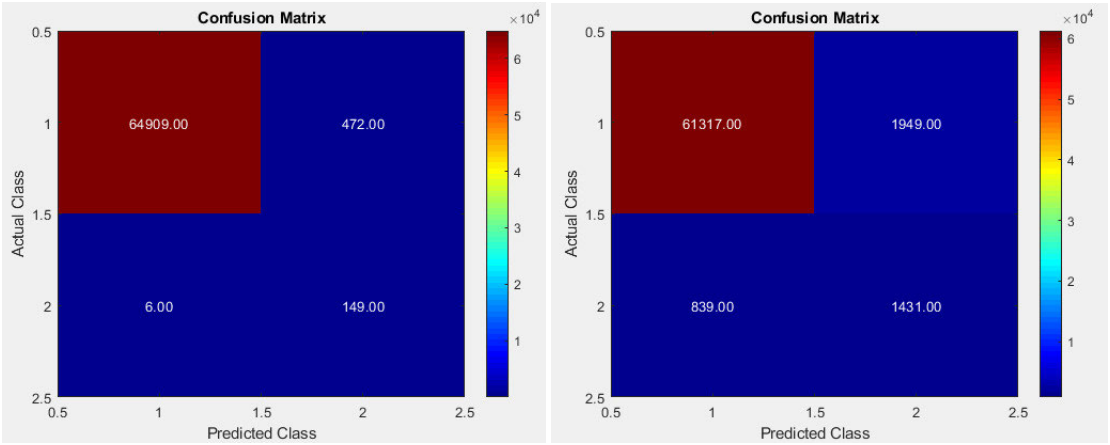

FIGURE 13. Confusion Matrix of random selected Images sets of brain different brain tumor types.

through statistical analysis. Most of these researchers have validated their method based on statistical measures such as mean, standard deviation (STD), intensity correlation (IC), and peak signal-to-noise ratio (PSNR) to assess the brain tumor in brain MRI images. Performance comparison of the most used classifiers including K-Nearest Neighbor (KNN), Self-organizing Map (SOM), Genetic Algorithm (GA), Graph Convolutional Neural Network (GCNN), Kernel-Based Support Vector Machine (SVM) and our proposed method which is presented in the Table 4. The results show that our proposed method outperforms existing techniques, demonstrating its effectiveness in detecting brain tumors and accurately classifying tumor regions. Classification performance will be validated in the next section.

E. IMPACT OF IMAGE ENHANCEMENT TECHNIQUE ON CLASSIFICATION MODULE PERFORMANCE

The evaluation of image enhancement methods' impact on brain MRI image classification using the CE-MRI database involves assessing key metrics, including sensitivity (Sen), specificity (Spec), accuracy (Acc), and Dice Similarity Coefficient (DSC). This section aims to validate image classification performance with and without enhancement methods. These performance metrics gauge the effectiveness of our proposed classification methods, as presented in Table 5. The analysis reveals that our methods consistently yield significantly higher sensitivity, specificity, accuracy, and DSC values when image enhancement techniques are applied compared to when they are not. Sensitivity reflects the model's ability to scan and detect tumor regions uniformly, while specificity indicates its accuracy in identifying abnormal region pixels.

Additionally, DSC and accuracy offer insights into the overall performance of classifying abnormal regions across all types of tumors. Specifically, the ''Meningiomas Tumor Images'' category demonstrates a substantial improvement in sensitivity (Sen), increasing from 0.67 without enhancement to 0.99 with enhancement. Similar enhancements in performance are observed in the ''Gliomas Tumor Images'' and ''Pituitary Tumor Image'' categories. The model consistently achieves higher sensitivity, specificity, accuracy, and DSC when applied image enhancement techniques.

These noteworthy improvements in sensitivity, specificity, accuracy, and DSC strongly indicate that image enhancement techniques positively impact the classification model's ability to detect and categorize tumors in MRI images.

F. COMPARISON OF CLASSIFICATION MODULE PERFORMANCE

Many researchers use the different classifiers for the detection of brain tumors and their analysis is based on the statistical measurements of various parameters. The table 6 shows the

TABLE 7. Performance of exiting mr imaging segmentation methods.

Method	Year	Technique	Acc. (%)
[43]	2017	SVM	96.51
[44]	2019	Back propagation neural networks.	93.33
[45]	2019	Deep Wavelet Autoencoder (DWA) and Deep Neural Network (DNN).	96
[46]	2019	Generative Adversarial Networks (GANs)	91
[47]	2019	Convolutional neural network	91.2
[48]	2019	Convolutional neural network	97.87
[49]	2019	K-NN	86
[50]	2019	Deep LSTM	97.87
[51]	2019	FCM clustering algorithm	97.5
[52]	2019	SVM	99.8
[53]	2019	KM-FCM	97
[54]	2019	Convolutional Neural Network	92
[55]	2019	Convolutional Neural Network	99.34
[56]	2020	Extreme learning based on FCM	95
[57]	2020	convolutional Neural Network	95
[58]	2022	SVM	95.1
Proposed Method	2023	ICA-NN-SVM	98.9

comparison of different classifiers such as K-Nearest Neighbor (KNN), Self-organizing Map (SOM), Genetic Algorithm (GA), Graph Convolutional Neural Network (GCNN) and Kernel-Based SVM, is compared to our proposed method classifier known as ICA-NN-SVM. It is clearly observed that our proposed method outperforms the existing methods in terms of sensitivity, specificity and accuracy as well as we also compared the computation time, it is also validated that our proposed method exhibits the faster processing time as compared to existing methods.The effectiveness of the our proposed method in accurately detecting abnormal tumor regions is verified through statistical parameter analysis. Essential metrics such as sensitivity, specificity, and accuracy are derived from the confusion matrix. The confusion matrix of random selected images of our proposed method is shown in the Figure 13.

G. COMPARATIVE ANALYSIS WITH EXISTING WORK

To assess the effectiveness of our proposed method, we performed an extensive comparison with recent techniques developed between 2019 and present. The results of the performance evaluation are presented in table 7. It is analyzed that despite the numerous methods based on CNN or deep learning since 2019, their performance remains relatively low due to lack of data as well as proper training. This can be attributed to the limited innovation in treatment methods within these approaches. In contrast, our proposed method ICA-NN-SVM. This helps improve performance by improving consistency between different brain MRI image regions, leading to more accurate classification. Our future work will mainly focus on designing new methods to improve training data using machine learning techniques. Our objective is to surpass the performance of current methods in future implementations. By emphasizing innovation and leveraging advanced machine learning techniques, we aim to make significant strides in brain tumor classification.

VII. CONCLUSION

In this study, we introduced a pioneering two-module methodology for the analysis of brain tumors using MRI images. Our approach uniquely addresses the challenges of image quality enhancement and effective classification, aiming to revolutionize the field of brain tumor analysis. The initial module termed the 'Image Enhancement Technique for Brain MRI Images', focuses on refining image quality by employing a combination of machine learning and imaging techniques. Specifically, adaptive Wiener filtering, neural networks, and independent component analysis work collaboratively to enhance and normalize images. This pre-processing step optimally prepares the images for subsequent segmentation and classification tasks.

The second module of our approach provides robust validation for the image enhancement technique and performs two critical functions: segmentation and classification. The segmentation process effectively isolates and highlights tumor regions within the brain images, while the classification accurately categorizes tumors into specific types using support vector machines (SVM).

Evaluation of our method using a diverse CE-MRI database demonstrated considerable advancements in contrast and efficiency for differentiating tumor types. Notably, our approach achieved outstanding performance metrics, including an

average sensitivity, specificity, accuracy, and Dice score (DSC) of 0.99, 0.99, 0.989, and 0.981, respectively. Moreover, the speed of our method sets it apart from existing approaches, with an average processing time of 0.43 seconds, highlighting a unique blend of accuracy and computational efficiency.

It is evident from our results that our method outperforms contemporary methods in sensitivity, specificity, accuracy, and DSC. This underscores the potential of our two-module approach to impact brain tumor analysis through image enhancement and classification significantly. Looking ahead, there are promising avenues for further research based on our groundbreaking methodology. Integrating more advanced artificial intelligence techniques, such as deep learning models, holds the potential further to improve the accuracy and efficiency of brain tumor classification. Additionally, exploring multi-modal imaging data and incorporating a wider variety of tumor types and demographic ranges in the dataset could enhance the generalizability of the method.

In conclusion, our study lays the groundwork for a future where brain tumor detection and classification are significantly more precise, efficient, and widely applicable. By continuously refining and innovating our methodology, we envision contributing to improved global health outcomes in the field of brain tumor analysis

REFERENCES

[1] Z. Khazaei, E. Goodarzi, V. Borhaninejad, F. Iranmanesh, H. Mirshekarpour, B. Mirzaei, H. Naemi, S. M. Bechashk, I. Darvishi, R. E. Sarabi, and A. Naghibzadeh-Tahami, "The association between incidence and mortality of brain cancer and human development index (HDI): An ecological study," *BMC Public Health*, vol. 20, p. 1696, Nov. 2020.

[2] T. S. Armstrong, M. Z. Cohen, J. Weinberg, and M. R. Gilbert, "Imaging techniques in neuro-oncology," *Seminars Oncol. Nursing*, vol. 20, pp. 231–239, Nov. 2004.

[3] H. W. Kim, L. Van Assche, R. B. Jennings, W. B. Wince, C. J. Jensen, W. G. Rehwald, D. C. Wendell, L. Bhatti, D. M. Spatz, M. A. Parker, and E. R. Jenista, "Relationship of T2-weighted MRI myocardial hyperintensity and the ischemic area-at-risk," *Circulation Res.*, vol. 117, no. 3, pp. 254–265, 2015.

[4] W. Deng, Q. Shi, K. Luo, Y. Yang, and N. Ning, "Brain tumor segmentation based on improved convolutional neural network in combination with non-quantifiable local texture feature," *J. Med. Syst.*, vol. 43, no. 6, p. 152, 2019.

[5] A. Lundervold and A. Lundervold, "An overview of deep learning in medical imaging focusing on MRI," *Zeitschrift für Medizinische Physik*, vol. 29, no. 2, pp. 102–127, 2019.

[6] Y. Jiang, J. Hou, X. Xiao, and H. Deng, "A brain tumor segmentation new method based on statistical thresholding and multiscale CNN," in *Proc. Int. Conf. Intell. Comput.*, 2018, pp. 235–245.

[7] M. Hssayeni, "Computed tomography images for intracranial hemorrhage detection and segmentation," *Intracranial Hemorrhage Segmentation Using Deep Convolutional Model. Data*, vol. 5, no. 1, p. 14, Mar. 2020.

[8] T. A. Soomro and J. Gao, "Neural network based denoised methods for retinal fundus images and MRI brain images," in *Proc. Int. Joint Conf. Neural Netw. (IJCNN)*, Vancouver, BC, Canada, Jul. 2016, pp. 1151–1157.

[9] E. F. Badran, E. G. Mahmoud, and N. Hamdy, "An algorithm for detecting brain tumors in MRI images," in *Proc. Int. Conf. Comput. Eng. Syst.*, Nov. 2010, pp. 368–373.

[10] T. A. Soomro, L. Zheng, A. J. Afifi, A. Ali, S. Soomro, M. Yin, and J. Gao, "Image segmentation for MR brain tumor detection using machine learning: A review," *IEEE Rev. Biomed. Eng.*, vol. 16, pp. 70–90, 2023.

[11] A. Selvapandian and K. Manivannan, "Fusion based glioma brain tumor detection and segmentation using ANFIS classification," *Comput. Methods Programs Biomed.*, vol. 166, pp. 33–38, Nov. 2018.

[12] M. Sharif, J. Amin, M. Raza, M. Yasmin, and S. C. Satapathy, "An integrated design of particle swarm optimization (PSO) with fusion of features for detection of brain tumor," *Pattern Recognit. Lett.*, vol. 129, pp. 150–157, Jan. 2020.

[13] A. Kumar, M. Ramachandran, A. H. Gandomi, R. Patan, S. Lukasik, and R. K. Soundarapandian, "A deep neural network based classifier for brain tumor diagnosis," *Appl. Soft Comput.*, vol. 82, Sep. 2019, Art. no. 105528.

[14] F. Özyurt, E. Sert, E. Avci, and E. Dogantekin, "Brain tumor detection based on convolutional neural network with neutrosophic expert maximum fuzzy sure entropy," *Measurement*, vol. 147, Dec. 2019, Art. no. 106830.

[15] A. R. Raju, P. Suresh, and R. R. Rao, "Bayesian HCS-based multi-SVNN: A classification approach for brain tumor segmentation and classification using Bayesian fuzzy clustering," *Biocybern. Biomed. Eng.*, vol. 38, no. 3, pp. 646–660, 2018.

[16] B. Yin, C. Wang, and F. Abza, "New brain tumor classification method based on an improved version of whale optimization algorithm," *Biomed. Signal Process. Control*, vol. 56, Feb. 2020, Art. no. 101728.

[17] A. Krol and B. Gimi, "Medical imaging 2017: Biomedical applications in molecular, structural, and functional imaging," in *Society of Photo-Optical Instrumentation Engineers*. Bellingham, WA, USA: SPIE, 2017.

[18] M. Mittal, L. M. Goyal, S. Kaur, I. Kaur, A. Verma, and D. J. Hemanth, "Deep learning based enhanced tumor segmentation approach for MR brain images," *Appl. Soft Comput.*, vol. 78, pp. 346–354, May 2019.

[19] M. A. Mohammed, M. K. Abd Ghani, R. I. Hamed, D. A. Ibrahim, and M. K. Abdullah, "Artificial neural networks for automatic segmentation and identification of nasopharyngeal carcinoma," *J. Comput. Sci.*, vol. 21, pp. 263–274, Jul. 2017.

[20] A. Rehman, S. Naz, M. I. Razzak, F. Akram, and M. Imran, "A deep learning-based framework for automatic brain tumors classification using transfer learning," *Circuits, Syst., Signal Process.*, vol. 39, pp. 757–775, Sep. 2020.

[21] M. K. Abd-Ellah, A. I. Awad, A. A. M. Khalaf, and H. F. A. Hamed, "Two-phase multi-model automatic brain tumour diagnosis system from magnetic resonance images using convolutional neural networks," *EURASIP J. Image Video Process.*, vol. 2018, no. 1, p. 97, 2018.

[22] N. Abiwinanda, M. Hanif, S. T. Hesaputra, A. Handayani, and T. R. Mengko, "Brain tumor classification using convolutional neural network," in *Proc. World Congr. Medical Phys. Biomed. Eng.*, vol. 1. Prague, Czech Republic: Springer, 2019, pp. 183–189.

[23] A. Pashaei, H. Sajedi, and N. Jazayeri, "Brain tumor classification via convolutional neural network and extreme learning machines," in *Proc. 8th Int. Conf. Comput. Knowl. Eng. (ICCKE)*, Oct. 2018, pp. 314–319.

[24] A. Gumaei, M. M. Hassan, M. R. Hassan, A. Alelaiwi, and G. Fortino, "A hybrid feature extraction method with regularized extreme learning machine for brain tumor classification," *IEEE Access*, vol. 7, pp. 36266–36273, 2019.

[25] S. Samarth R Phaye, A. Sikka, A. Dhall, and D. Bathula, "Dense and diverse capsule networks: Making the capsules learn better," 2018, *arXiv:1805.04001*.

[26] M. M. Badža and M. Č. Barjaktarović, "Classification of brain tumors from MRI images using a convolutional neural network," *Appl. Sci.*, vol. 10, no. 6, p. 1999, 2020.

[27] M. Sharma, G. N. Purohit, and S. Mukherjee, "Information retrieves from brain MRI images for tumor detection using hybrid technique K-means and artificial neural network (KMANN)," in *Networking Communication and Data Knowledge Engineering* (Lecture Notes on Data Engineering and Communications Technologies), vol. 4. G. Perez, K. Mishra, S. Tiwari, and M. Trivedi, Eds. Singapore: Springer, 2018, doi: 10.1007/978-981-10-4600-1_14.

[28] R. R. Monika and A. Kamboj, "Brain tumor classification for MR imaging using support vector machine," in *Progress in Advanced Computing and Intelligent Engineering* (Advances in Intelligent Systems and Computing), vol. 714, C. Panigrahi, A. Pujari, S. Misra, B. Pati, and K. C. Li, Eds. Singapore: Springer, 2019, doi: 10.1007/978-981-13-0224-4_16.

[29] R. Torres-Molina, C. Bustamante-Orellana, A. Riofrío-Valdivieso, F. Quinga-Socasi, R. Guachi, and L. Guachi-Guachi, "Brain tumor classification using principal component analysis and kernel support vector machine," in *Proc. 20th Int. Conf. Intell. Data Eng. Automated Learn.* Manchester, U.K.: Springer, 2019, pp. 89–96.

[30] T. A. Soomro, N. A. Jandan, A. Ali, M. Irfan, S. Rahman, W. A. Aldhabaan, A. S. Khairallah, and I. Abuallut, "Impact of retinal vessel image coherence on retinal blood vessel segmentation," *Electronics*, vol. 12, no. 2, p. 396, 2023.
[31] Y. E. Almalki, N. A. Jandan, T. A. Soomro, A. Ali, P. Kumar, M. Irfan, M. U. Keerio, S. Rahman, A. Alqahtani, S. M. Alqhtani, M. A. M. Hakami, S. A. Saeed, W. A. Aldhabaan, and A. S. Khairallah, "Enhancement of medical images through an iterative mccann retinex algorithm: A case of detecting brain tumor and retinal vessel segmentation," *Appl. Sci.*, vol. 12, no. 16, p. 8243, 2022.
[32] L. I. Rudin and S. Osher, "Nonlinear total variation based noise removal algorithms," *Physica D, Nonlinear Phenomena*, vol. 60, no. 1, 1992, Art. no. 259268.
[33] K. Debakla and M. Benyettou, "Image restoration using multilayer neural networks with minimization of total variation approach," *IJCSI Int. J. Comput. Sci. Issues*, vol. 383, no. 1, pp. 424–432, 2014.
[34] J. Sen, "Digital image enhancement and noise filtering by use of local statistics," *IEEE Trans. Pattern Anal. Mach. Intell.*, vol. PAMI-2, no. 2, pp. 165–168, Mar. 1980.
[35] A. Hyvarinen, "Fast and robust fixed-point algorithms for independent component analysis," *IEEE Trans. Neural Netw.*, vol. 10, no. 3, pp. 626–634, May 1999.
[36] Y. Matsuda and K. Yamaguchi, "Gram-schmidt orthonormalization to the adaptive ICA function for fixing the permutation ambiguity," in *Proc. Int. Conf. Neural Inf. Process.* Cham, Switzerland: Springer, 2016, pp. 152–159.
[37] R. Vankdothu and M. A. Hameed, "Brain tumor segmentation of MR images using SVM and fuzzy classifier in machine learning," *Meas., Sensors*, vol. 24, Dec. 2022, Art. no. 100440.
[38] C. Jun, "Brain tumor dataset," Figshare Dataset, Jun. 2017, doi: 10.6084/m9.figshare.1512427.v5.
[39] H. A. Vrooman, C. A. Cocosco, F. van der Lijn, R. Stokking, M. A. Ikram, M. W. Vernooij, Monique M. B. Breteler, and W. J. Niessen, "Multi-spectral brain tissue segmentation using automatically trained k-nearest-Neighbor classification," *Neuroimage*, vol. 37, no. 1, pp. 71–81, 2007.
[40] T. Logeswari and M. Karnan, "An improved implementation of brain tumor detection using segmentation based on hierarchical self organizing map," *Int. J. Comput. Theory Eng.*, vol. 2, no. 4, pp. 591–595, 2010.
[41] A. Kharrat, K. Gasmi, M. B. Messaoud, N. Benamrane, and M. Abid, "A hybrid approach for automatic classification of brain MRI using genetic algorithm and support vector machine," *Leonardo J. Sci.*, vol. 17, no. 1, pp. 71–82, 2010.
[42] A. K. Mandle, S. P. Sahu, and G. Gupta, "Brain tumor segmentation and classification in MRI using clustering and kernel-based SVM," *Biomed. Pharmacol. J.*, vol. 15, no. 2, pp. 699–716, Jun. 2022.
[43] N. B. Bahadure, A. K. Ray, and H. P. Thethi, "Image analysis for MRI based brain tumor detection and feature extraction using biologically inspired BWT and SVM," *Int. J. Biomed. Imag.*, vol. 2017, Mar. 2017, Art. no. 9749108.
[44] P. Mohamed Shakeel, T. E. El. Tobely, H. Al-Feel, G. Manogaran, and S. Baskar, "Neural network based brain tumor detection using wireless infrared imaging sensor," *IEEE Access*, vol. 7, pp. 5577–5588, 2019.
[45] P. Kumar Mallick, S. H. Ryu, S. K. Satapathy, S. Mishra, G. N. Nguyen, and P. Tiwari, "Brain MRI image classification for cancer detection using deep wavelet autoencoder-based deep neural network," *IEEE Access*, vol. 7, pp. 46278–46287, 2019.
[46] C. Han, L. Rundo, R. Araki, Y. Nagano, Y. Furukawa, G. Mauri, H. Nakayama, and H. Hayashi, "Combining noise-to-image and image-to-image GANs: Brain MR image augmentation for tumor detection," *IEEE Access*, vol. 7, pp. 156966–156977, 2019.
[47] M. Li, L. Kuang, S. Xu, and Z. Sha, "Brain tumor detection based on multimodal information fusion and convolutional neural network," *IEEE Access*, vol. 7, pp. 180134–180146, 2019.
[48] T. Hossain, F. S. Shishir, M. Ashraf, M. A. Al Nasim, and F. Muhammad Shah, "Brain tumor detection using convolutional neural network," in *Proc. 1st Int. Conf. Adv. Sci., Eng. Robot. Technol. (ICASERT)*, May 2019, pp. 1–6.
[49] S. N. Qasem, A. Nazar, A. Qamar, S. Shamshirband, and A. Karim, "A learning based brain tumor detection system," *Comput., Mater. Continua*, vol. 59, no. 3, pp. 713–727, 2019.
[50] J. Amin, M. Sharif, M. Raza, T. Saba, R. Sial, and S. A. Shad, "Brain tumor detection: A long short-term memory (LSTM)-based learning model," *Neural Comput. Appl.*, vol. 32, no. 20, pp. 15965–15973, Oct. 2020.
[51] M. S. Alam, M. M. Rahman, M. A. Hossain, M. K. Islam, K. M. Ahmed, K. T. Ahmed, B. C. Singh, and M. S. Miah, "Automatic human brain tumor detection in MRI image using template-based K means and improved fuzzy c means clustering algorithm," *Big Data Cognit. Comput.*, vol. 3, no. 2, p. 27, May 2019.
[52] S. Janardhanaprabhu and V. Malathi, "Brain tumor detection using depth-first search tree segmentation," *J. Med. Syst.*, vol. 43, no. 8, pp. 1–12, Aug. 2019.
[53] P. Rajan and C. Sundar, "Brain tumor detection and segmentation by intensity adjustment," *J. Med. Syst.*, vol. 43, no. 8, pp. 1–13, 2019.
[54] S. Pereira, A. Pinto, V. Alves, and C. A. Silva, "Brain tumor segmentation using convolutional neural networks in MRI images," *IEEE Trans. Med. Imag.*, vol. 35, no. 5, pp. 1240–1251, May 2016.
[55] N. Noreen, S. Palaniappan, A. Qayyum, I. Ahmad, M. Imran, and M. Shoaib, "A deep learning model based on concatenation approach for the diagnosis of brain tumor," *IEEE Access*, vol. 8, pp. 55135–55144, 2020.
[56] M. Sharif, J. Amin, M. Raza, M. A. Anjum, H. Afzal, and S. A. Shad, "Brain tumor detection based on extreme learning," *Neural Comput. Appl.*, col. 43, p. 282, Jul. 2020.
[57] P. Saxena, A. Maheshwari, and S. Maheshwari, "Predictive modeling of brain tumor: A deep learning approach," *Innovations in Computational Intelligence and Computer Vision* (Advances in Intelligent Systems and Computing), vol. 1189, M. K. Sharma, V. S. Dhaka, T. Perumal, N. Dey, and J. M. R. S. Tavares, Eds. Singapore: Springer, 2021, doi: 10.1007/978-981-15-6067-5_30.
[58] E. M. Senan, M. E. Jadhav, T. H. Rassem, A. S. Aljaloud, B. A. Mohammed, and Z. G. Al-Mekhlafi, "Early diagnosis of brain tumour mri images using hybrid techniques between deep and machine learning," *Comput. Math. Methods Med.*, vol. 2022, May 2022, Art. no. 8330833.

ABDULLAH A. ASIRI received the Ph.D. degree in medical imaging from the Centre for Advanced Imaging, The University of Queensland, Australia. He has more than 13 years of academic experience (since 2010) in teaching and research. Currently, he is an Associate Professor with the Radiological Sciences Department, Najran University, Saudi Arabia. His research interests include neuroimaging and diagnostic radiology, especially MRI. He was the Chairperson of the Radiological Sciences Department, from 2019 to 2023. He acted as the Vice Dean for the Academic Affairs with the College of Applied Medical Sciences, for one year. He is currently the Director of Scholarships with Najran University. He is also the Founder of MRI Saudi and a member of several national and international radiology societies.

TOUFIQUE AHMED SOOMRO (Senior Member, IEEE) received the Ph.D. degree in AI and image processing from Charles Sturt University, Australia, in 2018. Currently, he is an Associate Professor and the Head of the Department of Electronic Engineering, The University of Larkano, Pakistan. He is an accomplished academic with expertise in engineering and artificial intelligence (AI). He has made significant contributions to the field, with 61 research publications in AI for medical imaging. He has collaborated on projects related to AI for biomedical imaging with the Ministry of Education, Saudi Arabia, and Najran University. Additionally, he was honored as a Young Research Professor with Guangdong University of Technology, China, from 2019 to 2020. With his extensive knowledge and research expertise, he continues to advance the field of AI and image processing. As an Educator, he inspires students and contributes to the growth of electronic engineering. His accomplishments demonstrate his commitment to research excellence and his contributions to the scientific community. His research interests include image enhancement, segmentation, classification, and analysis for medical images.

AHMED ALI SHAH (Senior Member, IEEE) received the Bachelor of Engineering (B.E.) degree in electronic engineering from Mehran University of Engineering and Technology, Jamshoro, in 2010. In 2012, he received the prestigious Higher Education Commission (HEC) Pakistan fully funded HRDI-UET/USTPs Scheme Scholarship, for the M.S. studies leading to the Ph.D. studies from Hanyang University's Education Research Industry Cluster Ansan (E.R.I.C.A) Campus, South Korea. He has around eight years of diverse experience in academia, industry, and research. Over the past few years, he has participated in several industrial projects and received various technical training and certifications. He has hands-on experience in the soft fabrication of photonic-based sensing and imaging nanoplatforms, specifically his focus was to improve the limit of detection values (LODs), that in turn enhances sensitivity and minimizes safety risks. His research interests include surface-enhanced Raman scattering (SERS)-based sensing and imaging, anisotropic electric field responsive nanostructures, and smart sensors. To date, his research work has been disseminated to international audiences, in the form of patents, book chapters, SCI research journals articles, and peer-reviewed international conference proceedings.

GANNA POGREBNA is a pioneer of behavioural data science. She is currently the Executive Director of the Artificial Intelligence and Cyber Futures Institute, Charles Sturt University; an Honorary Professor with The University of Sydney; and the Lead for Behavioural Data Science with The Alan Turing Institute. Her expertise blends behavioral science, AI, computer science, data analytics, and business innovation. Her work aids diverse groups, including businesses, governments, and individuals, in understanding decision-making processes and optimizing behavior for enhanced outcomes. Her recent projects span smart technologies, cybersecurity, human–computer interactions, and innovative business models. Notably, her work in cybersecurity, particularly her CyberDoSpeRT scale, has gained international recognition. His contributions have earned her prestigious awards, including the Leverhulme Research Fellowship and the TechWomen100 Award. She is also recognized as a Leading Data Scientist by the *AI Time Journal*. She actively disseminates her knowledge through her Data Driven YouTube channel (https://www.youtube.com/@datadrivenchannel/videos) and Inclusion AI blog (https://inclusionai.org/), contributing to *The Oxford Handbook of Ethics of AI*and co-editing the upcoming *Handbook of Behavioural Data Science* (Cambridge).

MUHAMMAD IRFAN received the Ph.D. degree in electrical and electronic engineering from Universiti Teknologi PETRONAS, Malaysia, in 2016. He has two years of industry experience (October 2009–October 2011) and six years of academic experience (since January 2017) in teaching and research. Currently, he is an Associate Professor with the Electrical Engineering Department, Najran University, Saudi Arabia. He has authored more than 200 research papers in reputed journals, books, and conference proceedings (Google Scholar Citations of 2400 and H-index of 22). His research interests include automation and process control, energy efficiency, condition monitoring, vibration analysis, artificial intelligence, the Internet of Things (IoT), big data analytics, smart cities, and smart healthcare.

SAEED ALQAHTANI received the Ph.D. degree in medical imaging from the University of Dundee. He has more than eight years of academic experience (since 2013) in teaching and research. Currently, he is an Assistant Professor with the Radiological Sciences Department, Najran University, Saudi Arabia. His ResearchGate Citations is 45, R-score is 27.7, and an H-index is three. His research interests include diagnostic radiology, especially MRI and prostate MRI imaging. He is a member of SINAPSE (Scottish Imaging Network).